

**Overview and extension of Annexes D, E, F, regarding structural failure criteria, stability and nailed particle board to wood joints**

van der Put, Tom

**Publication date**  
2015

**Published in**  
Delft Wood Science Foundation publicaton series 2015

**Citation (APA)**

van der Put, T. (2015). Overview and extension of Annexes D, E, F, regarding structural failure criteria, stability and nailed particle board to wood joints. In *Delft Wood Science Foundation publicaton series 2015* (Vol. 5). (Delft Wood Science Foundation publicaton series; No. 5).

**Important note**

To cite this publication, please use the final published version (if applicable).  
Please check the document version above.

**Copyright**

Other than for strictly personal use, it is not permitted to download, forward or distribute the text or part of it, without the consent of the author(s) and/or copyright holder(s), unless the work is under an open content license such as Creative Commons.

**Takedown policy**

Please contact us and provide details if you believe this document breaches copyrights.  
We will remove access to the work immediately and investigate your claim.

## Overview and extension of Annexes D, E, F, regarding structural failure criteria, stability and nailed particle board to wood joints

T.A.C.M. van der Put  
Delft Wood Science Foundation  
Technical University Delft

### Overview annexes D: Structural failure criteria of wood structures

#### Introduction

The developed exact theory is given in the appended publications denoted by D, thus: **D(1991)**, **D(2008a)**, **D(2008b)**, **D(2010)**, **D(2011)**, **D(2012a)** **D(2012b)** and primary, by the partly expired **D(2006a)**, **D(2006b)**. Other relevant derivations and applications are mentioned in these publications. The theory in all appended publications was derived by T.A.C.M. van der Put as theory of perfect plasticity. Because a complete loading history analysis, with gradual increasing plasticity, until collapse is too extended and not necessary for ultimate state estimation, the relatively simple limit analysis method can always be applied instead. Then, no matter how complex the geometry of a problem, or loading condition, is, it is always possible to obtain a realistic value of the collapse load. This basic theory is discussed in the next section: D-1.

#### D-1. Upper and lower bound limit analysis of wood structures

The ultimate state represents a variational extremum problem and thus is based on small geometrical changes (using undeformed dimensions in the equilibrium equations). Because of the small changes, the virtual work equations apply. Because the top of a loading curve can be reached in many ways, differing an internal equilibrium system from each other, the previous loading history is not involved in the determination of the extremum and it is possible to use a linear- full plastic loading diagram for limit analysis (as is applied e.g. in exact fracture mechanics **C(2011b)**). In Fig.D-1, a scheme of the loading curve is given with a boundary (the elastic limit, depending on loading rate, temperature, etc.) where below the behavior can be assumed to be elastic (especially after mechanical conditioning) and where above the gradual flow of components at peak stresses and micro-cracking may have a similar effect as plastic flow with a hardening history up to the ultimate failure stress. The total main plane loading curves due to flow, damage and hardening behavior at any deformation rate, temperature, moisture content, loading history etc., up to flow and failure, fully can be described by deformation kinetics (see Annex B). When this loading curve is followed to a chosen or real ultimate stress point and then unloaded, the elastic and “plastic” deformation is known of that limit point. (The “plastic” amount (permanent strain in Fig.D-1 depends on the past, unknown, loading history at growth, drying, manufacturing, transport and pre-testing).

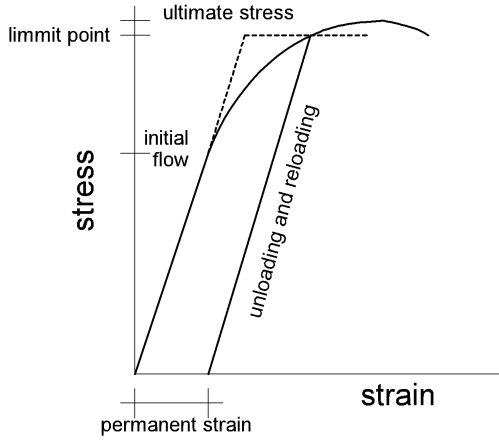


Fig.D-1. Loading curve

On reloading, the curve is elastic up to the limit point and it is possible to regard an elastic – full plastic description of the loading line according to the dashed line in Fig.D-1 as an allowable displacement field in the sense of limit analysis (that needs not to be the real occurring displacement for the virtual work equations). Also a reduced stiffness can be chosen as done for the Building Codes.

The virtual work equation, represents the extremum condition that the first variation of the potential energy is zero. Thus a small variation of the total potential energy vanishes when the structure is in equilibrium. Thus the total work of an equilibrium system is zero for any virtual displacement. The virtual work equation thus is based on an equilibrium set and a compatible set, which need not, and should not, be related. Thus:

$$\int_A T_i \dot{u}_i^* dA + \int_V F_i \dot{u}_i^* dV = \int_V \sigma_{ij} \dot{\epsilon}_{ij}^* dV, \quad (D-1)$$

integrated over the whole area  $A$  and volume  $V$  of the body.  $T_i$  and  $F_i$  are external forces on surface and in the body;  $\sigma_{ij}$  are the stresses, in equilibrium with the external forces, which need not to be the real actual occurring stresses. The asterisk is used for the compatible set, to emphasize that the two sets are not related, thus are completely independent.

A valid equilibrium set must satisfy the equilibrium equations:

$$\frac{\partial \sigma_{ji}}{\partial x_j} + F_i = 0 \quad (D-2)$$

and the equilibrium conditions at the load applications points (as boundary condition).

Of the compatible set, are the strains  $\dot{\epsilon}_{ij}^*$  compatible with real or imagined (virtual)

displacement rate  $\dot{u}_i^*$  of the points of application of the external forces, following the strain and displacement rate compatibility equation.

$$2\dot{\epsilon}_{ij}^* = \frac{\partial \dot{u}_i^*}{\partial x_j} + \frac{\partial \dot{u}_j^*}{\partial x_i} \quad (D-3)$$

Virtual displacements are not real, they can be physically impossible but they must be compatible with the geometry of the original structure and they must be small enough so that the original geometry is not significantly altered.

As equilibrium set, also the load increments can be used giving the rate equation:

$$\int_A \dot{T}_i \dot{u}_i^* dA + \int_V \dot{F}_i \dot{u}_i^* dV = \int_V \dot{\sigma}_{ij} \dot{\epsilon}_{ij}^* dV. \quad (D-4)$$

In the linear-full plastic schematization is the plastic zone a line in Fig.D-2, but is a plane in

stress space. Plastic flow occurs when the yield function  $f(\sigma_{ij}) = 0$  is satisfied. It is necessary that:

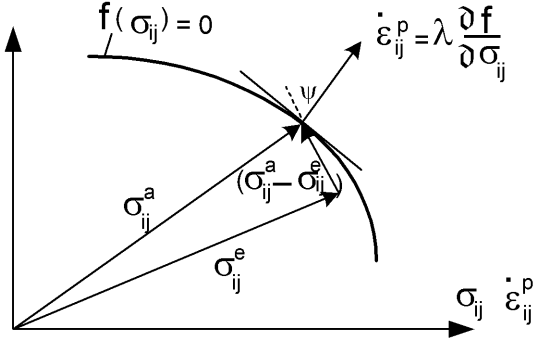


Fig.D-2 Yield surface and flow rule

$$(\sigma_{ij}^a - \sigma_{ij}^c) \cdot \dot{\epsilon}_{ij}^p \geq 0, \quad (D-5)$$

Thus this dot product is always positive and shows an angle  $\psi \leq 90^\circ$ , because thermodynamical real work (and real dissipation) has to be positive. Eq.(D-5) only is for all cases fulfilled when the vector  $\dot{\epsilon}_{ij}^p$  is perpendicular to the curve  $f(\sigma_{ij}) = 0$ , thus is in the direction of  $\partial f / \partial \sigma_{ij}$ . This is the convexity requirement or normality rule wherefore the principle of maximal local energy dissipation applies for the actual stress state, i.e. the projection in fig.D-2, of vector  $\sigma_{ij}^a$  on  $\dot{\epsilon}_{ij}^p$  is then maximal, higher than such projection of any other critical vector. In that case also the zero value of eq.(D-5) is reached for the plastic stress increment. Thus for the plastic flow increment then is:

$$\dot{\sigma}_{ij} \cdot \dot{\epsilon}_{ij}^p = 0 \quad (D-6)$$

From eq.(D-4) and (D-6) follows, that when the limit load is reached and the deformation proceeds under constant load, all stresses remain constant and only plastic, (not elastic) increments of strain occur. Because at collapse, eq.(D-4) becomes:

$$\int_A \dot{T}_i^c \dot{u}_i^c dA + \int_V \dot{F}_i^c \dot{u}_i^c dV = \int_V \dot{\sigma}_{ij}^c \dot{\epsilon}_{ij}^c dV. \quad (D-7)$$

With  $\dot{T}_i^c = \dot{F}_i^c = 0$ , and with elastic and plastic parts of strain,  $\dot{\epsilon}_{ij}^c = \dot{\epsilon}_{ij}^{ec} + \dot{\epsilon}_{ij}^{pc}$  is eq.(D-7):

$$\int_V \dot{\sigma}_{ij}^c \dot{\epsilon}_{ij}^c dV = \int_V \dot{\sigma}_{ij}^c (\dot{\epsilon}_{ij}^{ec} + \dot{\epsilon}_{ij}^{pc}) dV = \int_V \dot{\sigma}_{ij}^c (\dot{\epsilon}_{ij}^{ec}) dV = 0 \quad (D-8)$$

because of eq.(D-6), and thus  $\dot{\sigma}_{ij}^c \dot{\epsilon}_{ij}^{ec} = 0$ . Thus the elastic strain increment and consequently, the elastic stress increment, are zero and all deformation is plastic. Thus the elastic characteristic plays no part in the collapse at the limit load.

Next it is possible to give the proof of the lower and upper bound theorems of limit analysis. The lower bound theorem states that, if an equilibrium distribution of stress  $\sigma_{ij}^E$ , covering the whole body, can be found, which balances the applied loads and is everywhere below yield  $f(\sigma_{ij}^E) < 0$ , then the body will not collapse.

To prove this, assume that it is false, then two collapse equations exist:

$$\int_A T_i^c \dot{u}_i^c dA + \int_V F_i^c \dot{u}_i^c dV = \int_V \sigma_{ij}^c \dot{\epsilon}_{ij}^c dV$$

$$\int_A T_i^c \dot{u}_i^c dA + \int_V F_i^c \dot{u}_i^c dV = \int_V \sigma_{ij}^E \dot{\epsilon}_{ij}^c dV$$

and consequently is, because all deformation is plastic:

$$\int_V (\sigma_{ij}^c - \sigma_{ij}^E) \dot{\epsilon}_{ij}^{pc} dV = 0, \quad (D-9)$$

and because according to eq.(D-5):  $(\sigma_{ij}^c - \sigma_{ij}^E) \dot{\epsilon}_{ij}^{pc} > 0$  for  $\sigma_{ij}^E$  below yield, eq.(D-9) cannot be true and the lower bound theorem is proved.

The upper bound criterion states that if a compatible mechanism of plastic deformation is found, which satisfies the displacement boundary conditions, then the loads, determined by equating the rate, at which the external forces do work, eq.(D-10):

$$\int_A T_i \dot{u}_i^{p*} dA + \int_V F_i \dot{u}_i^{p*} dV, \quad (D-10)$$

to the rate of internal dissipation, eq.(D-11):

$$\int_V D(\dot{\epsilon}_{ij}^{p*}) dV = \int_V \sigma_{ij}^p \dot{\epsilon}_{ij}^{p*} dV \quad (D-11)$$

will be either higher or equal to the actual limit load.

Again, assume the theorem false, and the computed loads to be less than the actual limit load, then the following equation should apply:

$$\int_A T_i \dot{u}_i^{p*} dA + \int_V F_i \dot{u}_i^{p*} dV = \int_V \sigma_{ij}^E \dot{\epsilon}_{ij}^{p*} dV \quad (D-12)$$

with  $\sigma_{ij}^E$  everywhere below yield. Because  $T_i$  and  $F_i$  follow from equating eq.(D-10) and eq.(11), it follows that:

$$\int_V (\sigma_{ij}^{p*} - \sigma_{ij}^E) \dot{\epsilon}_{ij}^{p*} dV = 0 \quad (D-13)$$

However, according to eq.(D-5)  $(\sigma_{ij}^{p*} - \sigma_{ij}^E) \dot{\epsilon}_{ij}^{p*} > 0$  for  $\sigma_{ij}^E$  below yield, what leads to a contradiction and thus to the proof of the upper bound theorem.

Some corollaries, to be mentioned, following from the lower bound theorem, are, that:

- Initial stress or deformation have no effect on the plastic limit or collapse load provided the geometry is essential unaltered. This is e.g. applied in **C(2014)**.
- The limit load, computed from a convex yield surface, which circumscribes the actual surface, will be an upper bound on the actual limit load. The limit load computed from an inscribed surface will be a lower bound of the actual collapse load. This last is applied in the derivations of e.g. **D(2008a)**, by using the, in the von Mises inscribed Tresca polynomial). The graphical proof of the lower and upper bound is as follows:

In fig.D-3 is the plastic strain increment  $\dot{\epsilon}_c$  normal to the failure surface and is vector  $\sigma_l$  just inside the surface. Index  $c$  stands for actual collapse load and index  $l$  indicates lower bound.

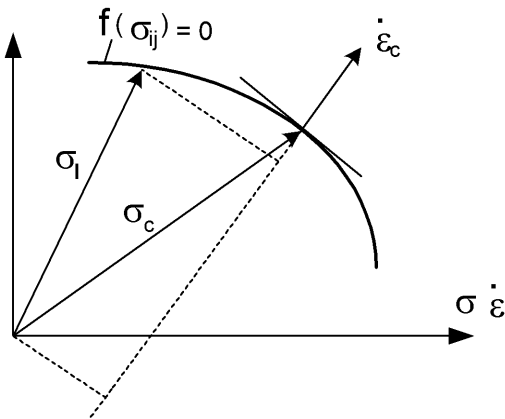


Fig.D-3. Proof of the lower bound theorem

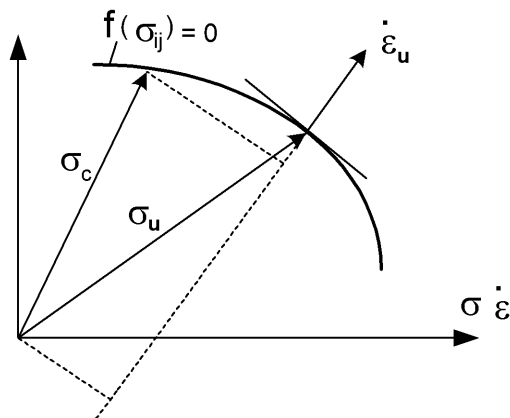


Fig.D-4. Proof of the upper bound theorem

According to the virtual work principle is for collapse:

$$\sum F_c \dot{w}_c = \int_V \sigma_c \dot{\epsilon}_c dV$$

and for a lower bound:

$$\sum F_l \dot{w}_c = \int_V \sigma_l \dot{\epsilon}_c dV$$

where  $F$  is the external force and  $w$  the displacement of  $F$ . The internal stress is  $\sigma_c$  with  $\dot{\epsilon}$  as strain increment. The dot product is the product of the strain increment with the components of the stress vector in the direction of strain increment. According to fig.D-3 is  $\sigma_l \dot{\epsilon}_c \leq \sigma_c \dot{\epsilon}_c$

thus is a lower bound due to the convexity of the yield function.

For the proof of the upper bound criterion applies, according to fig.D-4, that collapse must have occurred if:

$$\sum F_u \dot{w}_u = \int_V \sigma_u \dot{\epsilon}_u dV$$

According to the virtual work equation is: the upper bound criterion

$$\sum F_c \dot{w}_u = \int_V \sigma_c \dot{\epsilon}_u dV$$

The figure shows by projection of  $\sigma_u$  and  $\sigma_c$  on  $\dot{\epsilon}_u$  that:

$$\sigma_u \dot{\epsilon}_u \geq \sigma_c \dot{\epsilon}_u$$

Thus also  $F_u \geq F_c$  and  $F_u$  thus is the upper bound because of the convexity of the yield function.

## D-2. Derivation of the bearing strength perpendicular to grain of locally loaded timber blocks, D(2008a).

The theory of (practical unlimited) triaxial compressive strength is applied for several cases. The fundamental derivation is given in **D(2008a)** (and in the appendix of **D(1991)**). Based on the equilibrium method of plasticity, a stress field can be constructed in the plastic region of a specimen which satisfies the equilibrium conditions and boundary conditions and nowhere surmounts the failure criterion.

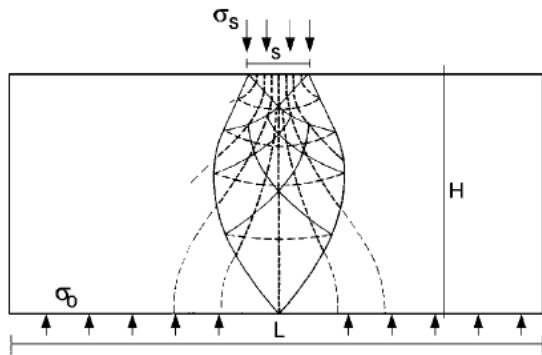


Fig.D-5. Shear direction lines of max. stress

This provides the theoretical explanation of the high bearing strengths of locally loaded timber blocks what is derived in the Appendices of **D(2008a)**. The resulting stress of this construction of an ultimate shear- or slip line field by the method of characteristics can precisely be represented by an analytical function of the outer logarithmic spiral slip line, which is the exact analytical solution.

This function in one variable, can be given in the power law form, leading to a theoretical

and experimental value of that power of 0.5. This power representation of the stress spreading model of the strength increase, by confined dilatation, provides simple rules for the code and a simple design method that precisely matches to the data in all circumstances and loading cases and explains the apparent contradictory test results of Suenson, the Eurocode, the French rules, Graf, Korin, Kollmann and Augustin et al., discussed in the Appendix of **D(1991)**, and, as shown before, explains other comparable loading cases of stress spreading as e.g. by nails and pin dowel connections, **F(2012a,b)**, **D(2008b)**. The slip-line field also provides an upper bound solution, which is as high as the lower bound solution and thus is equal to the real solution. As mentioned in the “Discussion of annexes A”, stress redistribution at initial failure of the matrix increases the compression stress in the matrix and increases the tensile stress in the reinforcement as hardening by stress redistribution, so that, by the high triaxial compression strength, matrix failure by compression, only can be in shear, thus according to the Tresca criterion.

The slip line solution is only a lower bound solution when also in the elastic regions, outside the plastic slip line region, the stress is low enough, below the ultimate value. This means that the ratio  $L/H$  should be just high enough to reach the same ultimate load as for longer blocks with higher  $L/H$  values. For shorter blocks,  $H$  of the plastic region should be limited to this lowest  $L/H$  value to obtain a lower bound solution. A safe method to find a sufficient low  $H$  for the ultimate state is to follow the spreading depth of the load of about 1.5 to 1. Thus for lower lengths  $L$ , the height  $H$  is limited and the slip line does not reach to the bottom of the block in order to have a real elastic state outside the slip lines. For ultimate load at initial flow, the St. Venant spreading 1 to 1 of the stresses in the isotropic matrix can be assumed, to have sufficient low stresses in the elastic area. This limitation of  $H$  depending on  $L$  and  $s$  is inserted in the theoretical formulas, providing a lower bound solution of the slip line construction. The theoretical formulas are not very sensitive for the assumed slopes also because of the adaptation of the Tresca value of these formulas to the measurements. The choice of  $H$  simply states a boundary condition for a lower bound solution by the theory. Based on theory, a correction is necessary according to: **D(2012a)**: “Restoration of exact design for partial compression perpendicular to the grain”. Code rules in the past always were based on the exact lower bound equilibrium method, but were replaced the last decennia by empirical rules, sometimes based on a few test-specimens without accounting the immense amount of data of other investigations. This also happened to the accepted and generally applied Eurocode rules given in the Appendix of **D(1991)**. To correct the new incorrect

empirical design rules for locally loaded beams and blocks of Eurocode 5, the necessary theoretical explanation of these rules and of the applied test data is given in **D(2012a)**. The by the coordinator of CIB-W18 given Eurocode rules, based on serviceability have nothing to do with the by him added test data. By putting them together a relation is suggested, but the tests are separate, full plastic, compression strength tests and the serviceability criterion is a, not related, arbitrarily chosen, criterion, not based on any investigation. It is shown in **D(2012a)** that such a criterion is mostly too safe, preventing the possibilities of most applications of wood but, in the same time, may be too unsafe for other boundary conditions. Instead of this Eurocode rule, the exact spreading rule has to be restored because this strength contains a necessary geometric factor as also applies e.g. for fracture mechanics and by volume effects of shear- tensile- and embedding strengths. As mentioned in **D(2012a)**, only a strength criterion has to apply and it is illegal, against European law, to apply a serviceability condition as strength criterion. The European agreement (pact) of not excluding reliable European products on national markets by additional serviceability requirements, prevents e.g. that a steel country may exclude building in wood by an additional requirement of compressibility equal to steel or that a wood country may prevent building in steel by the requirement of providing sufficient compressibility as applies to wood.

Because safety of people is a governmental issue, sufficient reliability now is necessary by European law. This only can be provided by applying exact theory, (the law of nature), which always can be applied accordingly to the lower bound equilibrium method of Limit analysis. Exact theory, means: derivation according to the scientific method, and verification of the derivation by all known published data and by predicting never measured behavior, which then has to be verified to be right by controlling test. That is why exact theory is able to predict design and never measured behavior with the right calculable reliability.

The failure data of the coordinator can not be analyzed because information of the tests is

Table II. Stress spreading factor:  $k_{c,90} = \sigma_{c,90,u}/f_{c,90} = 1.1 \cdot \sqrt{0.5 + 442/s}$  of Figure 2 data.

	1	2	3	4	5	6
Curve of Figure 2	$S$ (cm)	$f_{c,90}$ (MPa)	$k_{c,90}$ Equation 18	Theory $\sigma_{c,90,u}$ (MPa)	Measurements $\sigma_{c,90,u}$ (MPa)	Ultimate strain 6/178 (%)
1	18	1.6		1.6	1.6	3.4
2	18		1.89	3.0	3.0	3.4
3	12		2.25	3.6	3.3	3.4
5	7.9		2.72	4.3	4.3	3.4
6	5.5		3.21	5.2	5.4	3.4
7	1.4		6.23	10 < 9.6	> 7.5	> 1

Notes: Columns 4 and 5 show a precise fit of data to the spreading theory.

Curve 7 is cut off at 7.5 MPa in Figure 2. The theoretical value of 10 MPa is not met by the local failure mechanism:  $\sigma_{c,90,u} \leq 6 \cdot f_{c,90} = 6 \cdot 1.6 = 9.6$  MPa.

lacking. Even the beam-ends specimen form is not known. Probably this was a compression test on a specimen in the form of a beam end, what does not say anything on real failure modes of beams by combined loading cases. The failure has to be analyzed by the exact method and it is necessary to get information about these few tests, (with e.g. photos of the failure form), to show any relevance, because the rules have to be followed by whole Europe.

Since an extrapolated empirical rule is never identical to the theoretical description, the extrapolations are always unacceptably unreliable. This is shown and reported for the new rules of the Eurocode 5 to the Eurocode 5 Code-committee but did not pass the Dutch and German censorship against theory. Examples of abandoned theoretical approaches, which were initially accepted by the former CIB-W18 and Eurocode 5 Committee members are for example: **E(1990)**: Stability design, CIB-W18/23-15-2; **C(1990)**: Tension perpendicular, CIB-W18/23-10-1; **D(1991)**: Failure criterion + Appendix bearing strength, CIB-W18/24-6-1 and **A(1993)**: Failure criterion, CIB-W18/26-6-1. In **D(2012a)**, this replacement of theory by unsafe and uneconomical empirical rules is shown for design of locally loaded beams and blocks to make necessary corrections possible. Further, the necessary theoretical explanation

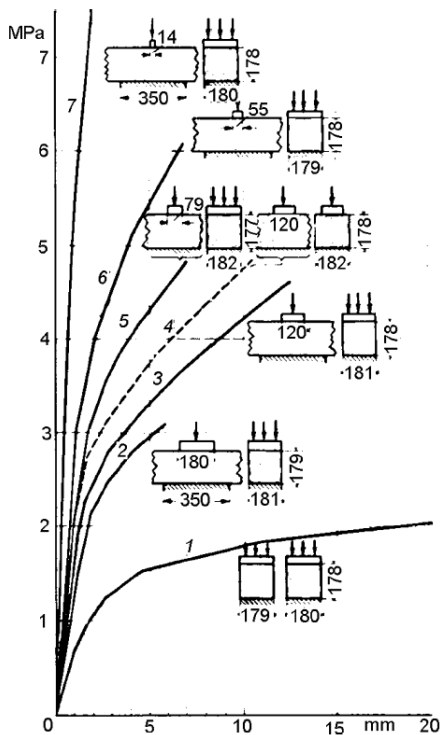


Fig.D-6. Spreading strength

of the applied empirical Eurocode 5 rules is not given and is derived in **D(2012a)**. This also was necessary because lack of possible correlation of the too limited data on which these rules are based. The data were e.g. deliberate restricted to only one spreading distance to deny the huge spreading effect of Fig.D-6. First in Section 2, the necessary derivation of the empirical Eurocode rule, Equation 1, of Blass and Gortlacher (2004) is given, leading to a new explanation of this empirically applied equation; which is based on the derivation of Madsen (see Madsen et al. 1982, discussed in Section 2.3 of **D(2012a)**). Next, in Section 3, the necessary theoretical analysis of the applied test results is given, followed in Appendix A by a retrieval of the earlier proposed; (theory based) Code rules which are in accordance with all known data and are applied since long in many countries. The theoretical derivation of the empirical Madsen equation is shown in Section 2 to apply only approximately (when extended and adapted) for very thin, long bearing blocks. This follows from the explanation of the constants, leading to an extended Madsen equation. This Madsen equation, thus, cannot be applied as general design and Eurocode rule. In contrast, it is shown by Table II of Section 3.1, (given above), that all strengths values of all loading lines of Fig.D-6, follow precisely the spreading equation from plasticity theory discussed in **D(2008a)**, and **D(2006b)**. This leads to the necessary application of the given, simple (already since 1991 generally applied) design rules of Appendix A of **D(1991)**, covering not only line 3, (following Blass and the Eurocode 5 rule) but all lines 1-7 in Fig.D-6 precisely and covering all the different lines of the other investigations as shown in **D(1991)** for the old Eurocode and French rules and for the measurements of Suenson and Graf, given in Kollmann (1984) and Korin (1990). Thus, the apparent contrary and totally different empirical results of all these different investigations are fully explained even by the simple power law representation of the exact theory of e.g. **D(2008a, 2008b, 2006b)** and **C(2000)**. This theory is based on the solution of the continuum mechanics boundary value problem by the method of characteristics. It is shown that the exclusion of the knowledge of the spreading effect in Eurocode 5 can be highly unsafe. This already occurred for example by measuring high embedding strengths on specimens with large nail distances and applying this to the low embedding strength structure by small nail distances. The reliable and economical design method, based on theory, demanded by European law, thus exists and is given for the first time in **D(1991)** and its Appendix B for locally loaded bearing blocks. For locally loaded

beams, design should be based on plasticity theory with the failure criterion for combined stresses, given in **A(2009)**. Design rules also exist in technical reports of the Stevin laboratory for pin-dowel joints, and in particle board, accounting for the possible very high embedding strength. This is common knowledge, already applied for over 30 years, (e.g. by the particle board industry). Concluding:

Based on the plasticity theory the theoretical explanation of the strength data is given **D(2008)**, **D(2006b)**. It is shown when the design rules are up to a factor 6 too conservative and when too unreliable. It also is shown why the Blassian premise and conclusion of no influence of the dimensions and depth of the test specimen on the strength is opposed by all other investigations and only applies for the chosen spreading free test specimen dimensions of his Eurocode investigation. It further is demonstrated, every 10 years, that the theory predicts and precisely explains and fits to all known data and provides a very simple reliable design rule for the Eurocode (given in Appendix B of **D(2008)**). The analysis further shows that design rules for bearing blocks don't apply unconditionally for support stresses on beams. This design has to be based on the failure criterion for combined stresses **D(2011)** showing that (except for unwanted early local failure due to under dimensioned bearing plates) the shear strength is determining for failure.

### D-3. Failure criterion for timber beams loaded in bending compression and shear

Limit analysis of beams is derived in: **D(2010)** and in **D(1991)**. Tests demonstrated a volume effect leading to a follow-up program, for combined loading,

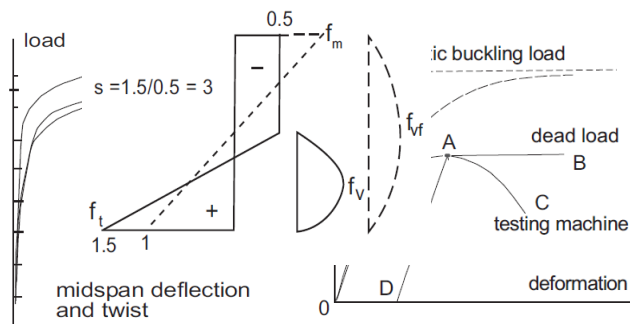
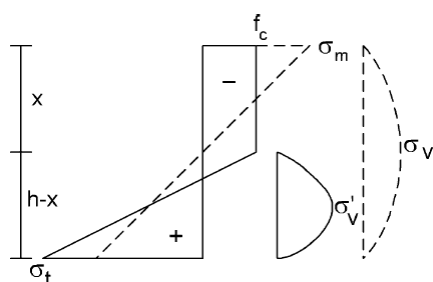


Fig. D-7. Loading lines and ultimate bending stress diagram on semi-full-scale glulam beams with the theoretically necessary perfect boundary conditions of the supports. There always occurred damage through lateral buckling, as follows from the cracking sounds during loading and the decreased (lateral) modulus of elasticity after unloading, even after the smallest possible lateral displacements and even for the most slender beams. The theory of elasticity in Chen and Atsuta (1972) does not show bifurcation for the three dimensional lateral buckling case, and the large displacements analysis (third order theory) shows a continuous rise in the loading curve (see fig.D-7). This means that the top of a loading curve always is due to damage and failure and therefore elastic buckling does not exist in praxis for the applied full size structural elements, as confirmed by the tests.



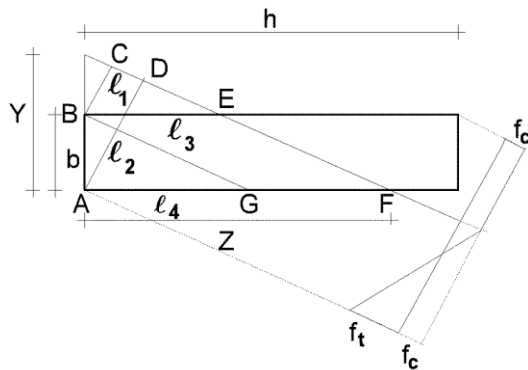
Stability design thus is a common second order strength calculation. The solutions of the second order equilibrium equations have to satisfy the failure criterion. This failure criterion is therefore essential and as shown in **A(2009)**, for statically indeterminate structures, and for combined loading, the idealized linear elastic calculation applied for failure, as given by the dashed lines in Fig.D-8, is not sufficient to describe and predict strength behavior and

needs to be replaced by the elastic-plastic calculation (solid lines in Fig.D-8).

The existing models and proposed design rules of the Eurocode 5 (2004) therefore have to be corrected in this way.

Now 3 different criteria are prescribed in the Eurocode for basically the same strength calculation: eq. 6.19, eq. 6.23 and eq. 6.35. This needs to be replaced by one equation of the real failure criterion (eq.D-5), which accounts for the elastic-plastic behavior of wood, showing unlimited bending and shear plastic flow in compression Fig. D-8 Ultimate stresses and brittle- stress, like behavior for tension.

$$\frac{6M}{f_m b h^2} = \frac{M}{M_{u,a}} = \left(1 - \frac{N}{N_u}\right) \left(1 + \frac{4N/N_u}{3s-1}\right) \quad (D-5)$$



The assumption of all existing models for combined bending and compression loading, that a specific compression strain limit is determining for failure is shown to be incorrect. For instance, it predicts from the compression failure that there is no size effect of the strength. The measurements and theory show that there always is a size effect at any value of  $s$  and for any load combination because the bending tensile strength is always

greater than the pure tension strength of the specimen. For this reason, bending tension failure always occurs, which leads to the starting point of unlimited flow in compression of the modified plasticity approach. The derived failure criterion for combined bending with compression is given by eq. (D-5). This equation can be approximated to two straight lines (eqs 15 and 16 of **D(2010)**), providing simple equations for design and for implementation of the Code. The derived failure criterion for combined shear with bending and compression is given by eq. (9). Because this line will give a cut-off of the ultimate bending-compression strength lines, this combined shear strength criterion always has to be checked, which should be in the Code. The size effect is lacking throughout the Blass model, giving questionable predictions of the strengths and an incorrect form of the interaction curves. The parabolic failure criterion of the failure criterion for timber beams, applied for Eurocode 5, is unsafe and denies the strong influence of quality and moisture content on the form of the curve (given by the parameter  $s$ ). The derived equation, eq.(21) shows the curvature along the beam to be a quadratic function of the bending stress, instead of a linear function, as is the incorrect basis of the existing approaches discussed in the previous section. Equation (21) provides a simple method for the ultimate second order bending moment estimation.

In **D(2012b)**, the derivation is given of the combined bi-axial bending, compression and shear strength of timber beams. As for other materials the elastic–full plastic limit design approach applies, which already is shown to precisely explain and predict uniaxial bending strength behavior. The derivation is based on choosing the location of the neutral line. This provides the stress distribution in the beam cross section in the ultimate state for that case, making it possible to calculate the associated ultimate bending moments in both main directions and ultimate normal- and shear

Fig. D-9. Bi-axial bending + compression.

force. The derived general equations are simplified to possible elementary design equations, applicable for building regulation.

In **D(2011)** **D(2006a)**, the derivation is given of the shear strength of continuous beams As continuation on the theoretical explanation of the bearing strengths of locally loaded

blocks, the bracing model is extended and it is shown that, with the right dimensioning, always the shear strength is determining. The elastic-plastic beam theory is extended for the influence of normal force and shear. Based on this extension the apparent contradictory test results of the shear- and bending strengths of beams and continuous beams is explained and also the shear and bracing action of beams loaded close to the supports is derived and verified by tests. It appears that the theory of elasticity is not able to explain the data and to give the right stress distribution in two span beams, underestimating the bearing capacity by a factor 2/3, while the elastic-plastic beam theory gives a very precise description of the data and the determining shear- and bending strengths. The derivations, confirmed by tests, lead to requirements for design rules of the Codes.

Thus the concluding final theory is published in two articles as:

1. "Failure criterion for timber beams loaded in bending, compression and shear", were based on the, for precise data explanation, necessary elastic-plastic strength calculation a derivation is given of the failure criterion for combined bending, compression and shear. This exact limit state criterion replaces the unacceptable unsafe criteria of the Eurocode 5, (EN 1995-1-1:2004)). It is shown that the thus far used principle of limited "flow" in axial compression as determining failure criterion, predicting e.g. no influence of a size effect, does not hold. Instead it is derived and confirmed by the data that bending tension failure is always determining showing the existence of a size effect and correction thus is necessary of the existing calculation method. Because the primary importance of the size effect for the strengths, also for combined bending- compression, a simple derivation of the size effect design equations is given and discussed.

2. "Derivation of the shear strength of continuous beams,

The elastic- full plastic loading curve is for all materials sufficient to explain the strength of beams and beam columns loaded by bending and compression. This theory is extended for the influence of shear stress and it is shown to be the only way to explain the combined bending-shear strength from test results. Also the in the past derived bearing strength theory is extended here for bracing action. It will be shown for continuous beams as example, that besides moment redistribution by plastic flow in bending, a plastic shear flow mechanism exists that also is able to cause full moment redistribution. The derivations lead to requirements for the design rules and show how the shear stress may reduce the ultimate bending capacity.

## **Overview Annexes E: Stability**

### **Introduction**

This publication is part of compilation of work of the author to a total rigorous theory, containing the latest developments with goal of a thesis and book. The appended articles are given in full as acknowledgment for the original journal publication.

The developed exact theory is given in the appended publications denoted by E, thus:

**E(1990)** and **E(2013)**. Other important derivations and applications are mentioned in these publications. The theory in all appended publications was derived by T.A.C.M. van der Put,

### **Discussion of annexes "E" about the exact stability criterion of wood**

In vdPut **E(1990)**, a general approach is given of the buckling and twist-bend buckling problem of symmetrical profiles loaded in bending in the two main directions and at the same time in torsion and compression. The model, according to the second order stress theory, provided a complete extension of the existing models by accounting for eccentrically lateral



building regulations. However exact theory is not able to pass the CIB-W18 censorship of the last decades. This lack of a demand of real theory causes, of course, the lack of knowledge of theory, as presented in the Annexes and e.g. of knowledge of elementary standard second order theory of buckling. This is not only demonstrated by the unacceptable Eurocode 5 design rules, but also by thesis work, (see E(2008a,b)) guided, for timber structures, by the CIB-W18 -coordinator. Despite of many written comments and discussions during years, it could not be prevented that the nonsense dissertation was written, what therefore is discussed in **E(2008a,b)** as warning for the chosen way to ridicule and destroy theory (see also D(2010)).

The given equations of the biaxial bending strength are in accordance with the limit analysis method and thus based on elastic-full-plastic behavior. Therefore, the analysis is rigorous and the strength prediction realistic and the result has to be applied in the Building Codes to provide the by Euro-law prescribed sufficient precise reliability calculation (also for the right prediction of behavior of totally new, never occurred and never measured, cases).

For the highest lower bound solution of biaxial bending strength, is necessary, that the neutral axis is a straight line, and that unlimited flow in pure compression occurs. Thus there is bending-tension failure and the shear stress is carried in the elastic part of the cross section. This is an improvement with respect to the thus far applied, (not unique) old model of Johns, and Buchanan, which is based on restricting the ultimate plastic compression strain at failure. The derived general expressions in coordinates of the boundary line of the full compression area provide 3 cases for design. For simplicity of design, is chosen for separate ultimate shear strength and ultimate bending-compression strength equations. The equations contain also the solution for uniaxial bending cases, which are already shown to precisely explain and fit data by the applied elastic full plastic limit analysis. The value of  $s = f_t / f_c$  appears to be about constant for all determining load combinations of bending with compression, indicating again (by the data of Johns and Buchanan) that there always is failure by the ultimate tensile strength. A volume effect by stress distribution thus needs not to be regarded as follows from the uniaxial data. The volume effect thus now is caused by the volume alone due to decreasing quality by volume increase.

The solutions of the most general equilibrium equations, eq.(54) and eq.(58) of **E(2013)** are exact, complete and universal, applicable for any material and load combination, based on the virtual work principle, which also is the basis of the lower and upper bound solutions of limit analysis and which always provides an exact solution however complex the equilibrium equations are. The equilibrium equations have to satisfy the mentioned biaxial failure criterion of the stability problem, which is always a strength problem for full scale timber beams as empirically verified in the past.

## **Overview of Annexes F: Nailed wood products to wood joints**

### **Introduction**

These publications are part of compilation of work of the author to a total theory according to the latest developments with possible goal of a thesis or a book. The appended articles are given in full as acknowledgment for the original journal publication. The developed exact theory is given in the appended 3 publications denoted by “F”, thus: vdPut **F(2008)**, **F(2012a)**, and **F(2012b)**. Other important derivations and applications are mentioned in these 3 publications. The theory in all appended publications was derived by T.A.C.M. van der Put.

### **F(2008): Explanation of the embedding strength of particle board**

By applying the earlier derived exact theory of the tri-axial embedding strength, **D(2006b)**

based on the exact method of limit analysis of plasticity, and by the derivation of the volume effect of the strength, it was possible to fully and precisely explain the empirical relations and test results of an extended investigation of the embedding strength of particle board, leading to a new insight for the right design rules, (which should be in Eurocode 5).

The basic theory of the embedding strength is given in: D(2008): "Derivation of the bearing strength perpendicular to the grain of locally loaded timber blocks"

The following is shown:

- The quasi linear dependence of the embedding strength on the density is explained. The 2 constants of the line have a constant ratio as explained by the theory.
- The high embedding strength is explained by confined dilatation due to the spreading effect as follows from the theory of plasticity.
- Splitting has no effect on spreading and therefore the embedding strength did not show an influence of the boundary conditions around the dowel (open or closed slit).
- Besides the plastic mechanism, a brittle splitting mechanism occurs at the dowel, explaining the volume effect for small dowels. Only due to this splitting, the succeeding embedment flow is possible.

The advantage of the power law approximation is that the powers of the spreading effect and of the volume effect can be summarized and the simple design equation is maintained.

- Based on the spreading and the volume effect, the empirical equations of the extended investigation of Budianto et al. (1977) can exactly be explained by the theoretical expressions. For instance, Eq. 18 explains as well the straight part as the curved part of the line of Fig. 4 and Eq. 26 explains the change of the slope of the lines of Fig. 5.
- The highest ultimate embedding strength is due to a local mechanism at the dowel as is verified in the TU-Delft investigation.
- The theory shows the embedding strength of Fig. 6 to be dependent on the  $b/d$  ratio and not on the  $a/d$  ratio of Fig. 3. This also follows from Dutch measurements at constant  $a/d$  with different  $b/a$  ratios. The verification of Eq. 9 or Eq. 27 follows from tests with one dowel diameter at different  $b/d$  ratios. These tests are lacking in Budianto et al. (1977) and it is necessary to adapt the Codes at these points for the right design.
- The theory and the TU-Delft investigation did show a very high embedding strength for nails with a limited working length due to 3-dimensional spreading.

### **F(2012) Nailed particle board to wood joints**

This is published at the Toronto Conference and given by two articles in one file F(2012):

1. Explanation of the strength particle board-to-wood joints with nails and staples
2. Estimation of the Influence of Rows of Nails in Particle Board to Wood Joints

Sub 1:

By the earlier derived theory of the embedding strength, based on limit design, it is possible to explain the extremely high embedding strength of nailed particle board to wood joints leading to a new exact failure equation for the embedding strength as necessary correction for design and for the Codes.

The following is shown:

- The stress spreading theory explains the high embedding strength for nails with a limited working length due to 3-dimensional spreading. The test-results confirm this behavior.
- The nail head reaction is important for spreading in thickness direction of the nailed particle board to wood plate. Stress spreading in thickness direction of the particle board plate can not be accounted for head-less nails.
- To account for this very high embedding strength of nailed particle board to wood joints, an iterative adaption for the spreading strength is derived, verified by test data.
- Also the derivation for a direct analytical estimation method of this high embedding

strength is given with the simplification of the formula and the very good fit to data is shown.

- Based on the local mechanism of fig. 4, the derivation is given of the highest possible ultimate embedding strength of particle board, which is verified by the discussed tests.

Sub 2:

The exact spreading theory, provides in article 1, the universal law of the embedding strength of nailed particle board to wood joints and even in the simplified power law form, this law is very precise. The consequence of the theory is that it also provides the right row factor for rows of nails, as is discussed in article 2, leading to a necessary application for design and for the Building Codes.

The following is shown:

- The stress spreading theory explains the high embedding strength for nails and the row factor for rows of nails. Test-results confirm this behavior.

- The test result of the designed critical specimen, which is critical for all different failure mechanisms (as combined bending–tension and shear failure of the plate with nail withdrawal) at the same time did indeed show the equal possibility of occurrence of all these mechanisms indicating the possibility of stress redistribution of the spreading stress and therefore no interaction of the failure mechanisms occurred (being all critical at about the same time).

- The derivation of the row factor is given, verified by data and a simplification for the Building Regulations is proposed.

- The necessary extension of the Johansen equation for nail head clamping and for stress spreading effect is given with the simplification of the formulas.

Correction factors of the strength for shorter nails are necessary.

All conclusions above also apply for nailed wood products to wood joints, when the wood products are quasi isotropic or are reinforced transverse to the nail loading direction (as e.g. wood, loaded perpendicular to grain or as plywood).